

## Supporting Information

### Theoretical study and application of 2-phenyl-1,3,4- thiadiazole derivatives with optical and inhibitory activity against SHP1

Chun Zhang<sup>a,#</sup>, Yi-Tao Sun<sup>a#</sup>, Li-Xin Gao<sup>a,b</sup>, Bo Feng<sup>a,b</sup>, Xue Yan<sup>a</sup>, Xue-Hui Guo<sup>d</sup>,  
Ai-Min Ren<sup>d\*</sup>, Yu-Bo Zhou<sup>b,c</sup>, Jia Li<sup>b,c\*</sup>, Wen-Long Wang<sup>a\*</sup>

<sup>a</sup>*School of Pharmaceutical Sciences, Jiangnan University, Wuxi, 214122, China. E-mail: [wwenlong2011@163.com](mailto:wwenlong2011@163.com)(W-L. W.)*

<sup>b</sup>*National Center for Drug Screening, State key Laboratory of Drug Research, Shanghai Institute of Materia Medica, Chinese Academy of Sciences, Shanghai, 201203, China. E-mail: [jli@simm.ac.cn](mailto:jli@simm.ac.cn)*

<sup>c</sup>*Zhongshan Institute for Drug Discovery, Shanghai Institute of Materia Medica, Chinese Academy of Sciences, SSIP Healthcare and Medicine Demonstration Zone, Zhongshan Tsuihang New District, Zhongshan, Guangdong528400*

<sup>d</sup>*Institute of Theoretical Chemistry, College of Chemistry, Jilin University, Liutiao Road 2#, Changchun 130061, P.R. China*

## Table of Contents

### Computational studies

Table S1. The optimized  $S_0$  and  $S_1$  geometries of all studied structures.

Table S2. The calculated one-photon absorption spectra of all the studied molecules at the level of TD-DFT//M06-2X/6-31+G(d)/SMD ( $H_2O$ ).

Table S3. The calculated two-photon absorption spectra of all the studied molecules at the level of Cam-B3LYP/6-31+G(d)/PCM( $H_2O$ ).

Table S4. TPA tensor elements ( $S_{ab}$ ) and TPA cross section ( $\sigma_{a.u.}$  in a.u.) of all the studied molecules by calculating at the Cam-B3LYP/6-31+G(d)/PCM ( $H_2O$ ) level.

Table S5. The calculated emission spectra of PT1–PT7 at the level of TD-DFT//B3LYP/6-31+G(d)/SMD( $H_2O$ ).

Table S6. The calculated emission spectra of PT1–PT7 at the level of TD-DFT//M06-2X/6-31+G(d)/SMD( $H_2O$ ).

Table S7. The calculated emission spectra of PT1–PT10 at the level of TD-DFT//M06-2X/6-31+G(d) with different solvent environment.

Table S8. The calculated fluorescence wavelength of PT8, PT9 and PT10 including state specific effect at the level of TD-DFT//M06-2X/6-31+G(d)/PCM( $H_2O$ ).

Figure S1. The comparison diagram of stable ground state  $S_0$  (green) and excited state  $S_1$  (red) for PT8, PT9 and PT10.

Figure S2. HR factors and crucial displacement vectors for the normal modes with large HR factors for PT9 and PT10.

### Experimental studies

S1. General procedure for the synthesis of compounds 3A – 3C and 4A – 4B.

S1.1 General procedure for the synthesis of compounds 2A – 2E

S1.2 General procedure for the synthesis of compounds 3A – 3E

S1.3 General procedure for the synthesis of compounds 3F – 3G

S1.4 General procedure for the synthesis of compounds 4A – 4B

NMR spectra

Figure S3. The UV excitation spectra of PT1- PT10 in PBS buffer (PBS: DMSO = 9:1) with a concentration of  $1.0 \times 10^{-4}$  M.

Figure S4. Fluorescence emission spectra of PT1- PT7 in PBS buffer (PBS: DMSO = 9:1) with a concentration of  $1.0 \times 10^{-4}$  M by excitation at 330 nm, 350 nm, 330 nm, 330 nm, 330 nm, 330 nm, 340 nm, respectively.

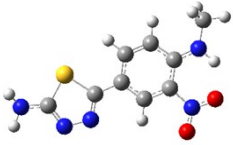
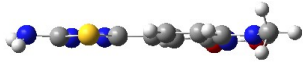
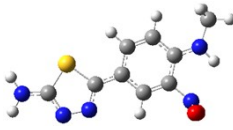
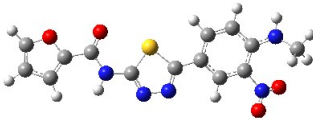
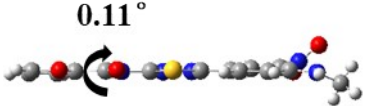
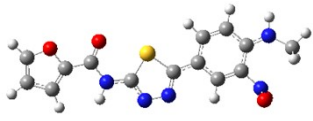
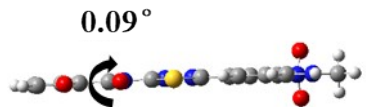
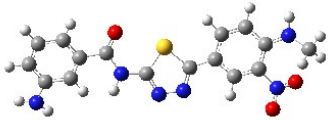
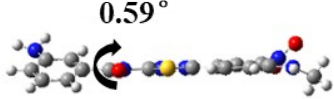
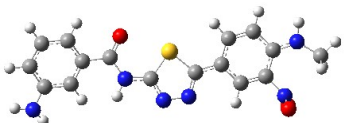
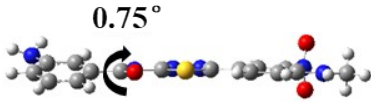
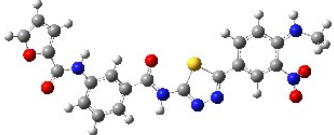
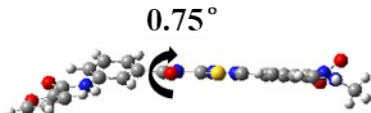
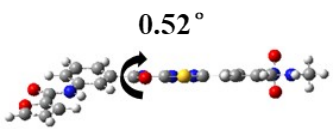
Table S8. Inhibitory activities of PT8, PT9 and PT10 against SHP1<sup>PTP</sup> and SHP2<sup>PTP</sup>, respectively.

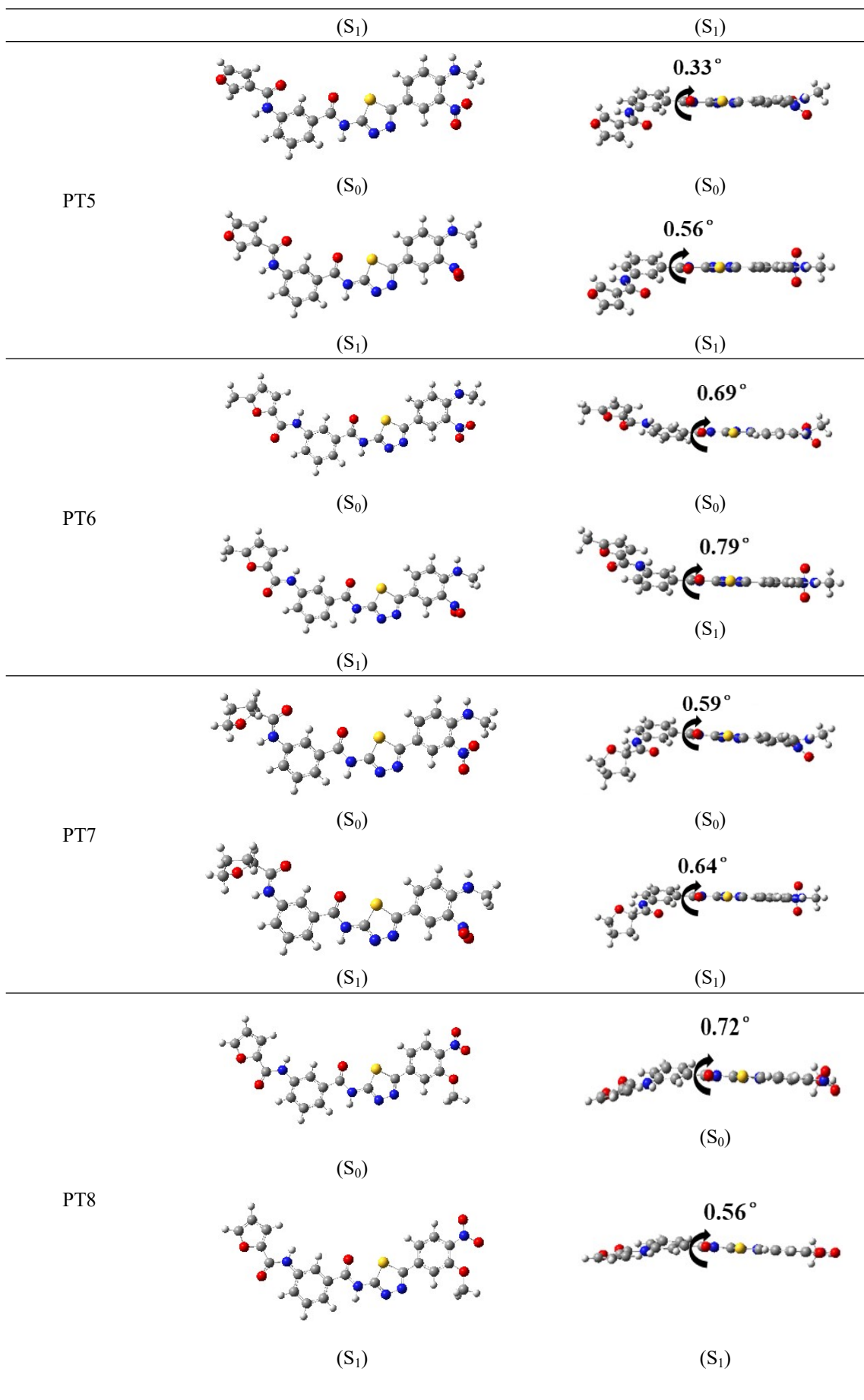
Figure S5. Time dependent/independent inhibition for SHP1<sup>PTP</sup> by NSC87877.

Figure S6. The fluorescence experiment of PT9 against the SHP1<sup>PTP</sup> and SHP2<sup>PTP</sup> enzyme activity.

## Computational studies

Table S1. The optimized  $S_0$  and  $S_1$  geometries of all studied structures.

Molecules	Top view	Side view
PT1	 ( $S_0$ )	 ( $S_0$ )
	 ( $S_1$ )	 ( $S_1$ )
PT2	 ( $S_0$ )	 $0.11^\circ$ ( $S_0$ )
	 ( $S_1$ )	 $0.09^\circ$ ( $S_1$ )
PT3	 ( $S_0$ )	 $0.59^\circ$ ( $S_0$ )
	 ( $S_1$ )	 $0.75^\circ$ ( $S_1$ )
PT4	 ( $S_0$ )	 $0.75^\circ$ ( $S_0$ )
	 ( $S_1$ )	 $0.52^\circ$ ( $S_1$ )



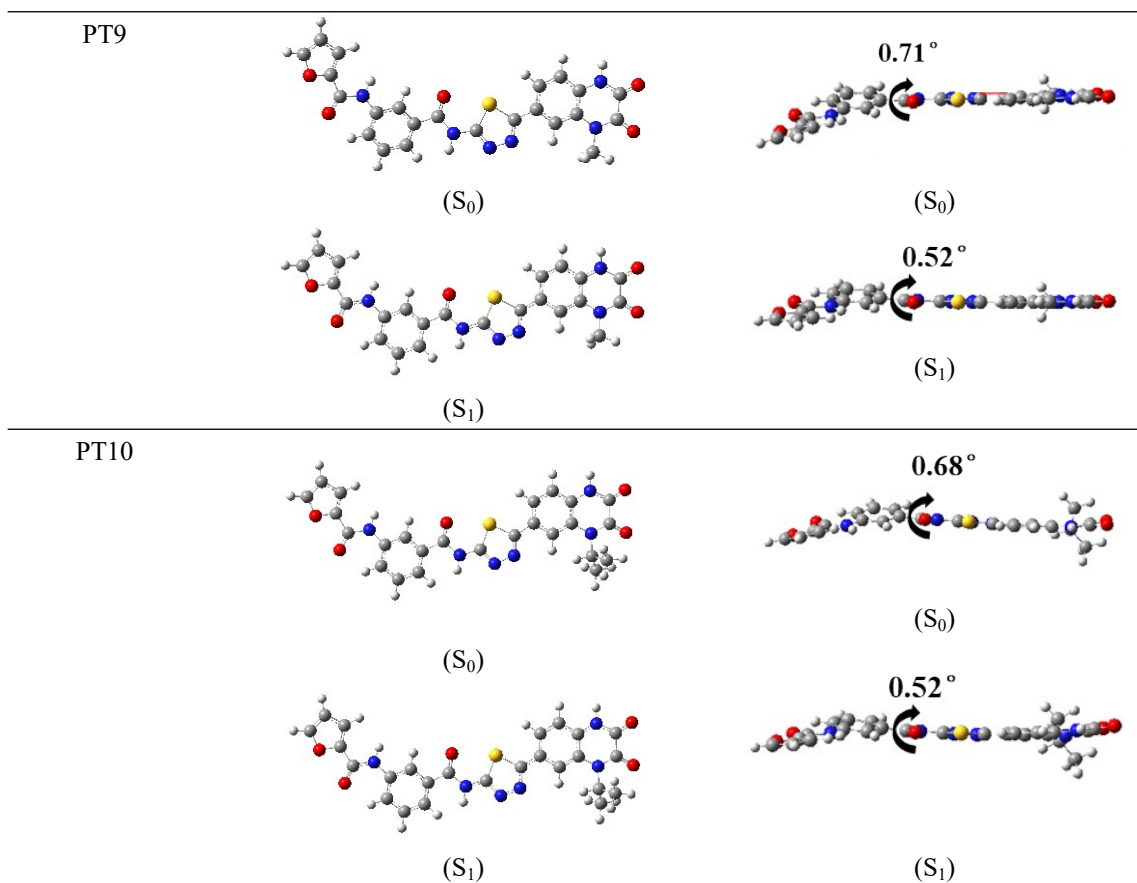


Table S2. The calculated one-photon absorption spectra of all the studied molecules at the level of TD-DFT//M06-2X/6-31+G(d)/SMD (H<sub>2</sub>O).

Molecules	$\lambda^{\text{OPA}}/\text{nm}$	<i>Osc.</i>	Transition natures
PT1	300.5	0.8441	S <sub>0</sub> →S <sub>3</sub> (H→L+1 94.73%)
PT2	316.6	1.2201	S <sub>0</sub> →S <sub>2</sub> (H→L+1 78.73%)
PT3	313.9	1.1208	S <sub>0</sub> →S <sub>2</sub> (H→L+1 77.38%)
PT4	315.4	1.2028	S <sub>0</sub> →S <sub>2</sub> (H→L+1 71.24%)
PT5	314.3	1.1312	S <sub>0</sub> →S <sub>2</sub> (H→L+1 73.84%)
PT6	328.1	1.3665	S <sub>0</sub> →S <sub>2</sub> (H→L+1 69.64%)
PT7	313.9	1.1040	S <sub>0</sub> →S <sub>2</sub> (H→L+1 73.73%)
PT8	336.8	0.4576	S <sub>0</sub> →S <sub>1</sub> (H-1→L 57.86%)
PT9	313.7	1.3986	S <sub>0</sub> →S <sub>1</sub> (H→L 82.94%)
PT10	312.5	1.3599	S <sub>0</sub> →S <sub>1</sub> (H→L 80.53%)

H represents highest occupied molecular orbital, while L is lowest unoccupied molecular orbital

Table S3. The calculated two-photon absorption spectra of all the studied molecules at the level of Cam-B3LYP/6-31+G(d)/PCM(H<sub>2</sub>O).

Molecules	$\lambda^{\text{TPA}}/\text{nm}$	Cross section /GM	Transition natures
PT1	624.7	26	S <sub>0</sub> →S <sub>2</sub>
PT2	620.9	81	S <sub>0</sub> →S <sub>2</sub>

PT3	645.8	79	$S_0 \rightarrow S_2$
PT4	647.5	101	$S_0 \rightarrow S_2$
PT5	645.8	93	$S_0 \rightarrow S_2$
PT6	647.5	99	$S_0 \rightarrow S_2$
PT7	644.2	92	$S_0 \rightarrow S_2$
PT8	702.5	65	$S_0 \rightarrow S_1$
PT9	580.8	75	$S_0 \rightarrow S_2$
PT10	580.8	70	$S_0 \rightarrow S_2$

Table S4. TPA tensor elements ( $S_{ab}$ ) and TPA cross section ( $\sigma_{a.u.}$  in a.u.) of all the studied molecules by calculating at the Cam-B3LYP/6-31+G(d)/PCM (H<sub>2</sub>O) level.

Molecules	Excited States	$S_{xx}$	$S_{yy}$	$S_{zz}$	$S_{xy}$	$S_{xz}$	$S_{yz}$	$\sigma_{a.u.}$
PT1	2	-0.1	-38.6	111.9	-0.0	-0.1	-12.4	67993
PT2	2	-0.1	17.0	-200.1	-0.9	4.3	4.1	228729
PT3	2	-0.1	14.5	-195.6	-1.8	1.7	-7.6	220056
PT4	2	-0.7	-6.4	213.3	6.4	9.0	43.1	283027
PT5	2	-2.9	-1.9	201.3	6.9	-1.1	-47.6	257876
PT6	2	-1.2	-4.2	209.3	6.6	-7.4	-47.1	276986
PT7	2	-5.4	-2.0	202.3	-9.6	6.5	-42.1	255060
PT8	1	-1.0	54.7	137.5	3.2	-4.1	-80.6	212899
PT9	2	-1.6	-3.3	166.4	-0.9	8.9	10.5	164496
PT10	2	0.5	-5.0	-159.4	-1.0	1.8	-7.3	155921

Table S5. The calculated emission spectra of PT1–PT7 at the level of TD-DFT//B3LYP/6-31+G(d)/SMD(H<sub>2</sub>O).

Molecules	$\lambda^{EMI}/nm$	<i>Osc.</i>	Transition natures
PT1	4877.3	0	$S_1 \rightarrow S_0$ (L→H 97.7%)
PT2	2426.0	0	$S_1 \rightarrow S_0$ (L→H 97.98%)
PT3	2378.3	0	$S_1 \rightarrow S_0$ (L→H 98.13%)
PT4	2361.3	0	$S_1 \rightarrow S_0$ (L→H 98.15%)
PT5	2341.3	0	$S_1 \rightarrow S_0$ (L→H 98.14%)
PT6	2338.7	0	$S_1 \rightarrow S_0$ (L→H 98.12%)
PT7	2378.5	0	$S_1 \rightarrow S_0$ (L→H 98.14%)

Table S6. The calculated emission spectra of PT1–PT7 at the level of TD-DFT//M06-2X/6-31+G(d)/SMD(H<sub>2</sub>O).

Molecules	$\lambda^{EMI}/nm$	<i>Osc.</i>	Transition natures	RMSD
PT1	527.6	0.2324	$S_0 \rightarrow S_1$ (L→H 93.11%)	0.137

PT2	776.7	0.0001	S <sub>0</sub> →S <sub>1</sub> (L→H 82.68%)	0.431
PT3	775.2	0.0002	S <sub>0</sub> →S <sub>1</sub> (L→H 83.13%)	0.398
PT4	774.3	0.0001	S <sub>0</sub> →S <sub>1</sub> (L→H 83.17%)	0.345
PT5	772.0	0.0001	S <sub>0</sub> →S <sub>1</sub> (L→H 83.18%)	0.439
PT6	773.7	0.0001	S <sub>0</sub> →S <sub>1</sub> (L→H 83.16%)	0.551
PT7	772.5	0.0001	S <sub>0</sub> →S <sub>1</sub> (L→H 83.22%)	0.413

The solvent effects for emission spectra were listed in Table S7 by calculating the fluorescence properties in different solvent environment. It demonstrated that: (1) solvent model (SMD or PCM) had small effect on the emission wavelength for all studied molecules. (2) The larger solvent polar (H<sub>2</sub>O > DMSO > DCM) led to longer emission wavelength, especially for PT1-PT8. According to compare the linear-response and state specific (*J. Chem. Phys.*, 2006, 125, 054103.) solvent effect for fluorescence (Table S7 and S8) of PT8, PT9 and PT10, it can be found that state specific solvent effect red-shifted fluorescence wavelength (underestimated the transition energy) of PT8, and blue-shifted fluorescence wavelength (overestimated the transition energy) of PT9 and PT10 compared with those of linear-response solvent model (in Table S7).

Table S7. The calculated emission spectra of PT1–PT10 at the level of TD-DFT//M06-2X/6-31+G(d) with different solvent environment.

Molecules	$\lambda^{\text{EMI}}/\text{nm}$	<i>Osc.</i>	Transition natures
PT1	517.8 <sup>a</sup>	0.1715 <sup>a</sup>	S <sub>0</sub> →S <sub>1</sub> (L→H 93.40%) <sup>a</sup>
	495.9 <sup>b</sup>	0.1612 <sup>b</sup>	S <sub>0</sub> →S <sub>1</sub> (L→H 93.52%) <sup>b</sup>
	492.4 <sup>c</sup>	0.1486 <sup>c</sup>	S <sub>0</sub> →S <sub>1</sub> (L→H 93.52%) <sup>c</sup>
PT2	774.0 <sup>a</sup>	0.0001 <sup>a</sup>	S <sub>0</sub> →S <sub>1</sub> (L→H 78.84%) <sup>a</sup>
	694.8 <sup>b</sup>	0.0001 <sup>b</sup>	S <sub>0</sub> →S <sub>1</sub> (L→H 78.92%) <sup>b</sup>
	679.9 <sup>c</sup>	0.0001 <sup>c</sup>	S <sub>0</sub> →S <sub>1</sub> (L→H 78.29%) <sup>c</sup>
PT3	770.3 <sup>a</sup>	0.0001 <sup>a</sup>	S <sub>0</sub> →S <sub>1</sub> (L→H 79.25%) <sup>a</sup>
	695.9 <sup>b</sup>	0.0001 <sup>b</sup>	S <sub>0</sub> →S <sub>1</sub> (L→H 79.29%) <sup>b</sup>
	684.3 <sup>c</sup>	0.0001 <sup>c</sup>	S <sub>0</sub> →S <sub>1</sub> (L→H 78.66%) <sup>c</sup>
PT4	765.5 <sup>a</sup>	0.0000 <sup>a</sup>	S <sub>0</sub> →S <sub>1</sub> (L→H 79.31%) <sup>a</sup>
	697.1 <sup>b</sup>	0.0001 <sup>b</sup>	S <sub>0</sub> →S <sub>1</sub> (L→H 79.29%) <sup>b</sup>
	681.8 <sup>c</sup>	0.0001 <sup>c</sup>	S <sub>0</sub> →S <sub>1</sub> (L→H 78.65%) <sup>c</sup>
PT5	763.7 <sup>a</sup>	0.0001 <sup>a</sup>	S <sub>0</sub> →S <sub>1</sub> (L→H 79.26%) <sup>a</sup>
	697.3 <sup>b</sup>	0.0001 <sup>b</sup>	S <sub>0</sub> →S <sub>1</sub> (L→H 79.26%) <sup>b</sup>
	685.7 <sup>c</sup>	0.0001 <sup>c</sup>	S <sub>0</sub> →S <sub>1</sub> (L→H 78.60%) <sup>c</sup>
PT6	765.9 <sup>a</sup>	0.0001 <sup>a</sup>	S <sub>0</sub> →S <sub>1</sub> (L→H 79.28%) <sup>a</sup>
	696.8 <sup>b</sup>	0.0001 <sup>b</sup>	S <sub>0</sub> →S <sub>1</sub> (L→H 79.32%) <sup>b</sup>
	681.5 <sup>c</sup>	0.0001 <sup>c</sup>	S <sub>0</sub> →S <sub>1</sub> (L→H 78.59%) <sup>c</sup>
	764.3 <sup>a</sup>	0.0001 <sup>a</sup>	S <sub>0</sub> →S <sub>1</sub> (L→H 79.25%) <sup>a</sup>

	699.7 <sup>b</sup>	0.0001 <sup>b</sup>	S <sub>0</sub> →S <sub>1</sub> (L→H 79.24%) <sup>b</sup>
	687.3 <sup>c</sup>	0.0001 <sup>c</sup>	S <sub>0</sub> →S <sub>1</sub> (L→H 78.57%) <sup>c</sup>
PT8	560.3 <sup>a</sup>	0.1707 <sup>a</sup>	S <sub>0</sub> →S <sub>1</sub> (L→H 78.62%) <sup>a</sup>
	663.1 <sup>b</sup>	0.1506 <sup>b</sup>	S <sub>0</sub> →S <sub>1</sub> (L→H 77.90%) <sup>b</sup>
	624.7 <sup>c</sup>	0.1604 <sup>c</sup>	S <sub>0</sub> →S <sub>1</sub> (L→H 77.85%) <sup>c</sup>
PT9	392.5 <sup>a</sup>	1.4566 <sup>a</sup>	S <sub>0</sub> →S <sub>1</sub> (L→H 94.33%) <sup>a</sup>
	396.9 <sup>b</sup>	1.4262 <sup>b</sup>	S <sub>0</sub> →S <sub>1</sub> (L→H 93.33%) <sup>b</sup>
	391.4 <sup>c</sup>	1.4241 <sup>c</sup>	S <sub>0</sub> →S <sub>1</sub> (L→H 93.23%) <sup>c</sup>
PT10	392.1 <sup>a</sup>	1.4706 <sup>a</sup>	S <sub>0</sub> →S <sub>1</sub> (L→H 92.98%) <sup>a</sup>
	396.7 <sup>b</sup>	1.4001 <sup>b</sup>	S <sub>0</sub> →S <sub>1</sub> (L→H 93.19%) <sup>b</sup>
	391.4 <sup>c</sup>	1.3977 <sup>c</sup>	S <sub>0</sub> →S <sub>1</sub> (L→H 92.52%) <sup>c</sup>

a: The results were computed using the solvent model and environment of PCM/H<sub>2</sub>O (a), SMD/DMSO (b) and SMD/DCM (c). H represents highest occupied molecular orbital, while L lowest unoccupied molecular orbital.

Table S8. The calculated fluorescence wavelength of PT8, PT9 and PT10 including state specific effect at the level of TD-DFT//M06-2X/6-31+G(d)/PCM(H<sub>2</sub>O).

Molecules	ΔE/eV	λ <sup>EMI</sup> /nm
PT8	2.05	603.8
PT9	3.33	371.9
PT10	3.32	373.0

Basing on the optimized geometries of excited state S<sub>1</sub> and ground state S<sub>0</sub>, the

root-mean-square deviation (RMSD) =  $\sqrt{\frac{1}{N} \sum_i [(x_i - x'_i)^2 + (y_i - y'_i)^2 + (z_i - z'_i)^2]}$  was calculated by PyMol software to compare the extent of the geometry distortion between the ground state minimum S<sub>0</sub> and excited state minimum S<sub>1</sub>.

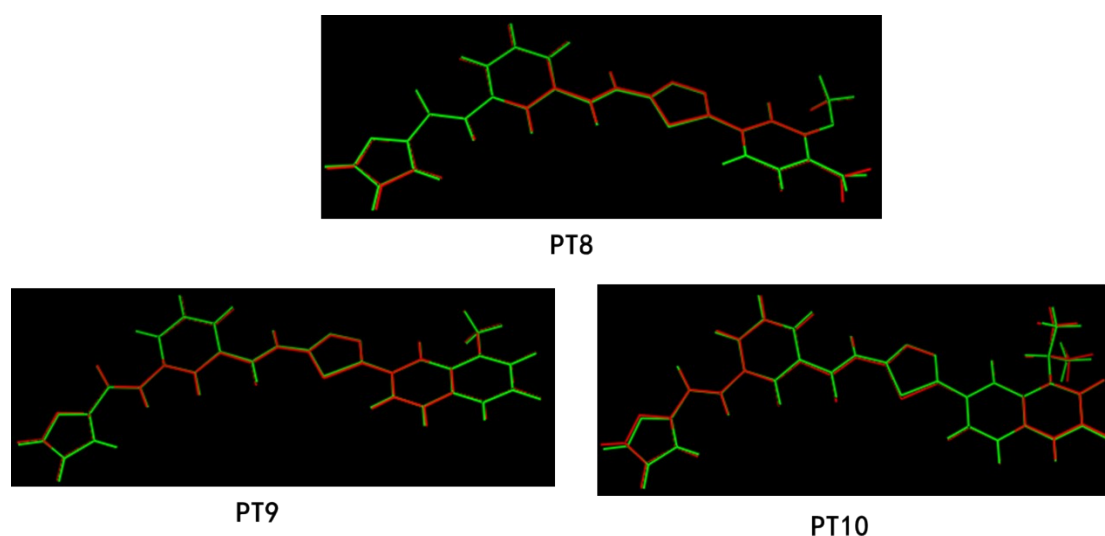


Figure S1. The comparison diagram of stable ground state S<sub>0</sub> (green) and excited state S<sub>1</sub> (red) for

PT8, PT9 and PT10.

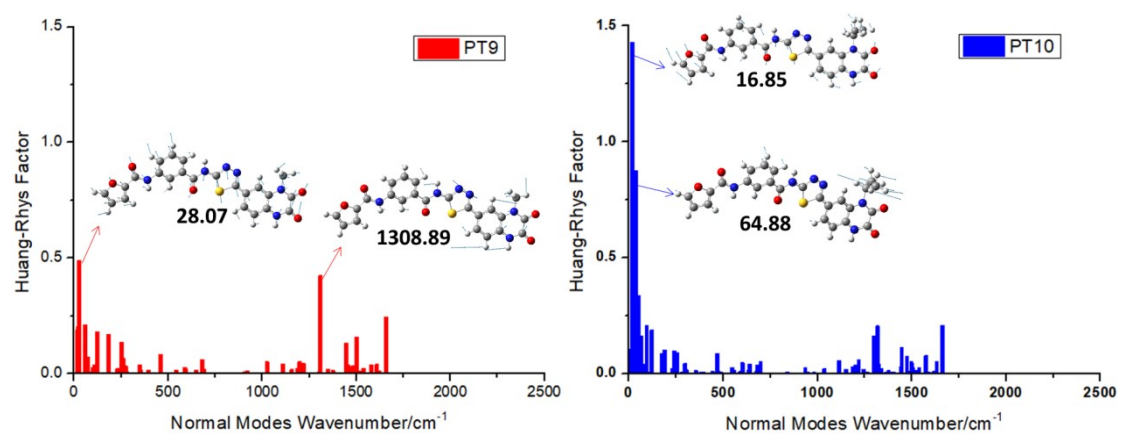


Figure S2. HR factors and crucial displacement vectors for the normal modes with large HR factors for PT9 and PT10.

## Experimental studies

All chemicals were reagent grade and used as purchased. <sup>1</sup>H NMR (400 MHz) spectra were recorded on a Bruker AVIII 400 MHz spectrometer. The chemical shifts were reported in (ppm) using the 2.50 signal of DMSO (<sup>1</sup>H-NMR) as internal standards and the 39.52 signal of DMSO (<sup>13</sup>C-NMR) as internal standards. ESI Mass spectra (MS) was obtained on Shimadzu LCMS-2020.

### **S1. General procedure for the synthesis of compounds 3A – 3C and 4A – 4B.**

#### **S1.1 General procedure for the synthesis of compounds 2A – 2E**

A solution of compounds **1A – 1E** (1.0 equiv, 5.6 mmol) and thiosemicarbazide (1.0 equiv, 5.6 mmol) in phosphorus oxychloride (10 mL) was heated at 80 °C for 12 h. When the reaction was completed, the reaction solution was quenched with ice-cold water (50 mL), and the mixture was adjusted to pH = 7 with saturated aqueous sodium bicarbonate solution. Then the reaction mixture was extracted with EtOAc (30 mL) and dried over anhydrous sodium sulfate. The crude product was concentrated under reduced pressure and purified by silica gel column chromatography (PE/EtOAc=91 : 9 ~ 50 : 50, *V* : *V*) to give compounds **2A – 2E**.

#### **S1.2 General procedure for the synthesis of compounds 3A – 3E**

A mixture of compounds **2A – 2E** (1.0 equiv, 1.4 mmol) and corresponding amidobenzoic acid (1.2 equiv, 1.7 mmol) was dissolved in DMF (4 mL) followed by addition of HATU (1.2 equiv, 1.7 mmol) and DIPEA (2.0 equiv, 2.8 mmol) consequently. Then the reaction was stirred at room temperature for 16 h. After the reaction was finished, water (30 mL) was added to the reaction solution, and the aqueous layer was extracted with EtOAc (20 mL) for 3 times. The combined organic layers were dried over anhydrous sodium sulfate and concentrated under reduced pressure. The crude product was purified by silica gel column chromatography (PE / EtOAc = 83 : 17 ~ 50 : 50, *V* : *V*) to give products **3A – 3E**.

*N*-(5-(4-(methylamino)-3-nitrophenyl)-1,3,4-thiadiazol-2-yl)furan-2-carboxamide(**3A**). Compound **3A** was prepared according to the general procedure and the product was obtained as pale red solid in 45% yield. <sup>1</sup>H NMR (400 MHz, DMSO-*d*<sub>6</sub>) δ: 8.46 (s, 1H), 8.38 (s, 1H), 8.07 (d, *J* = 8.4 Hz, 1H), 7.78 (s, 1H), 7.13 (d, *J* = 9.2 Hz, 2H), 6.58 (s, 1H), 3.03 (d, *J* = 4.8 Hz, 3H); MS (ESI) *m/z* calcd for C<sub>14</sub>H<sub>12</sub>N<sub>5</sub>O<sub>4</sub>S [M+H]<sup>+</sup> 346.1, found 346.1.

*N*-(3-((5-(4-(methylamino)-3-nitrophenyl)-1,3,4-thiadiazol-2-yl)carbamoyl)phenyl)furan-3-carboxamide(**3B**). Compound **3B** was prepared according to the general procedure and the product was obtained as pale red solid in 48% yield. <sup>1</sup>H NMR (400 MHz, DMSO-*d*<sub>6</sub>)  $\delta$ : 13.13 (s, 1H), 10.16 (s, 1H), 8.59 (d, *J* = 2.4 Hz, 1H), 8.49 (d, *J* = 5.6 Hz, 1H), 8.42 (s, 2H), 8.13 (dd, *J* = 8.8, 1.6 Hz, 1H), 8.03 (d, *J* = 8.4 Hz, 1H), 7.90 (d, *J* = 8.4 Hz, 1H), 7.82 (t, *J* = 1.6 Hz, 1H), 7.55 (t, *J* = 8.0 Hz, 1H), 7.17 (d, *J* = 9.2 Hz, 1H), 7.03 (d, *J* = 1.2 Hz, 1H), 3.04 (d, *J* = 5.2 Hz, 3H); MS (ESI) *m/z* calcd for C<sub>21</sub>H<sub>17</sub>N<sub>6</sub>O<sub>5</sub>S [M+H]<sup>+</sup> 465.1, found 465.1.

*N*-(3-((5-(3-methoxy-4-nitrophenyl)-1,3,4-thiadiazol-2-yl)carbamoyl)phenyl)furan-2-carboxamide(**3C**). Compound **3C** was prepared according to the general procedure and the product was obtained as pale red solid in 43% yield. <sup>1</sup>H NMR (400 MHz, DMSO-*d*<sub>6</sub>)  $\delta$ : 13.36 (s, 1H), 10.45 (s, 1H), 8.52 (s, 1H), 8.06-8.02 (m, 2H), 7.98 (d, *J* = 1.2 Hz, 1H), 7.92 (d, *J* = 8.0 Hz, 1H), 7.89 (d, *J* = 1.2 Hz, 1H), 7.73 (dd, *J* = 8.4, 1.6 Hz, 1H), 7.56 (t, *J* = 8.0 Hz, 1H), 7.39 (dd, *J* = 3.6, 0.8 Hz, 1H), 6.73 (q, *J* = 1.6 Hz, 1H), 4.08 (s, 3H); MS (ESI) *m/z* calcd for C<sub>21</sub>H<sub>16</sub>N<sub>5</sub>O<sub>6</sub>S [M+H]<sup>+</sup> 466.1, found 466.1.

### S1.3 General procedure for the synthesis of compounds **3F** – **3G**

To a solution of compounds **3D** – **3E** (1.0 equiv, 0.8 mmol) and SnCl<sub>2</sub> (3.0 equiv, 2.4 mmol) in EtOAc (5 mL) was added HCl (1 mL) dropwise. Subsequently the reaction mixture was stirred at 80 °C for 2 h under the nitrogen atmosphere. When the reaction was completed, the mixture was added to a saturated aqueous sodium bicarbonate solution (20 mL) for adjusting to pH = 7 and extracted with EtOAc (10 mL). The combined organic layers were dried over anhydrous sodium sulfate and concentrated under reduced pressure. The crude product was purified by silica gel column chromatography (DCM/MeOH=99 : 1 ~ 95 : 5, *V* : *V*) to give compounds **3F** – **3G**.

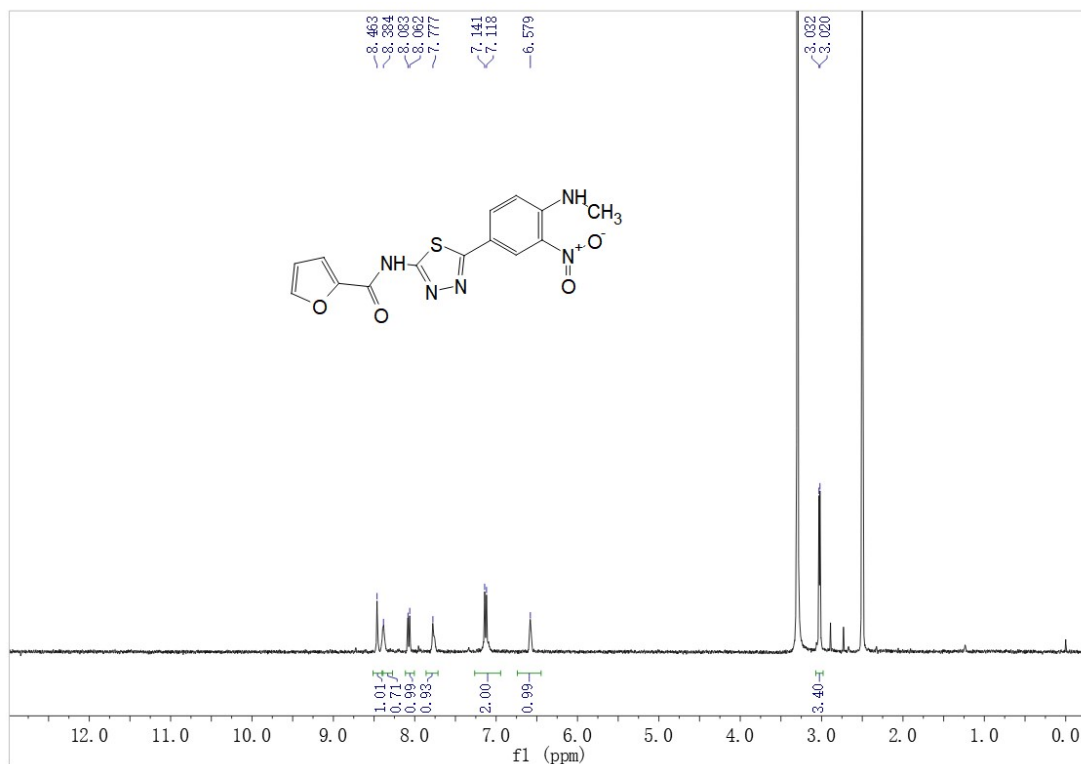
### S1.4 General procedure for the synthesis of compounds **4A** – **4B**

A solution of compounds **3F** – **3G** (1.0 equiv, 0.5 mmol) in diethyl oxalate (5.0 equiv, 2.2 mmol) was stirred at 120 °C for 16 h. After the reaction was completed, the reaction mixture was concentrated under reduced pressure. Then the crude product was purified by silica gel column chromatography (PE / EtOAc = 80 : 20 ~ 50 : 50, *V* : *V*) to give compounds **4A** – **4B**.

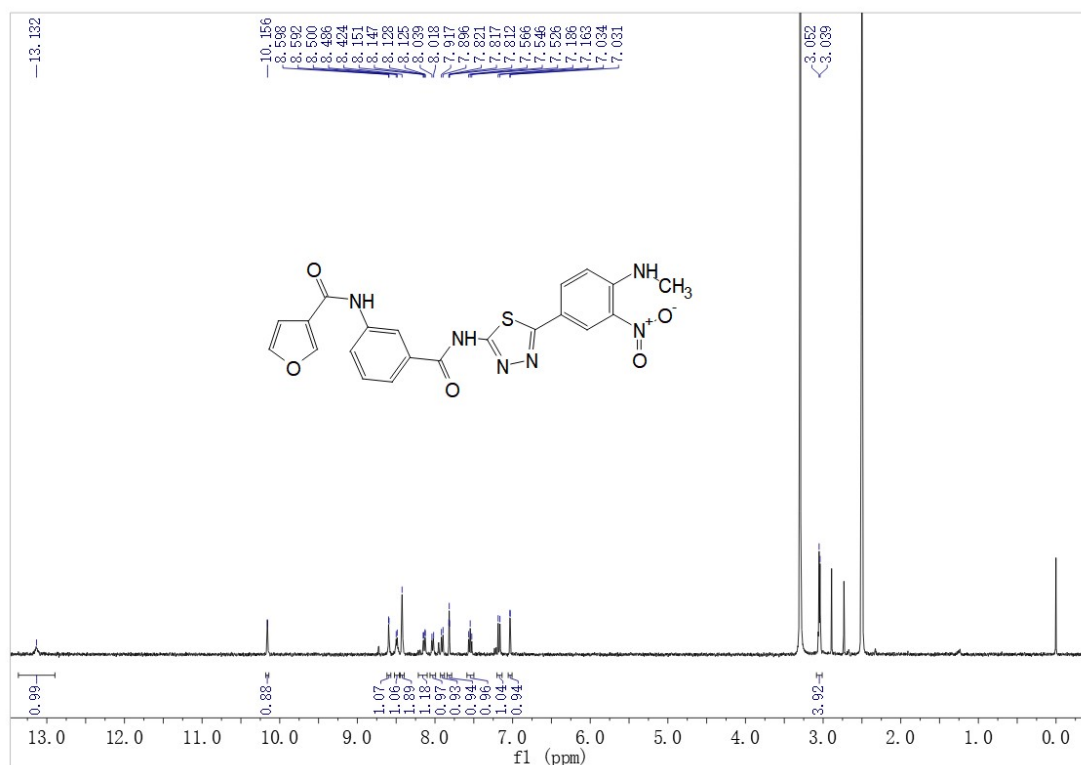
*N*-(3-((5-(1-methyl-2,3-dioxo-1,2,3,4-tetrahydroquinoxalin-6-yl)-1,3,4-thiadiazol-2-yl)carbamoyl)phenyl)furan-2-carboxamide(**4A**). Compound 4A was prepared according to the general procedure and the product was obtained as pale yellow solid in 56% yield. <sup>1</sup>H NMR (400 MHz, DMSO-*d*<sub>6</sub>) δ: 12.15 (s, 1H), 10.43 (s, 1H), 8.51 (s, 1H), 8.03 – 7.97 (m, 2H), 7.91 (d, *J* = 8.4 Hz, 1H), 7.82 – 7.76 (m, 2H), 7.57 – 7.49 (m, 2H), 7.40 (d, *J* = 3.2 Hz, 1H), 6.73 (dd, *J* = 3.2, 1.6 Hz, 1H), 4.26 (q, *J* = 6.8 Hz, 1H), 3.56 (s, 3H); MS (ESI) *m/z* calcd for C<sub>23</sub>H<sub>17</sub>N<sub>6</sub>O<sub>5</sub>S [M+H]<sup>+</sup> 489.1, found 489.1.

*N*-(3-((5-(1-isopropyl-2,3-dioxo-1,2,3,4-tetrahydroquinoxalin-6-yl)-1,3,4-thiadiazol-2-yl)carbamoyl)phenyl)furan-2-carboxamide(**4B**). Compound 4B was prepared according to the general procedure and the product was obtained as pale yellow solid in 52% yield. <sup>1</sup>H NMR (400 MHz, DMSO-*d*<sub>6</sub>) δ: 12.10 (s, 1H), 10.41 (s, 1H), 8.50 (s, 1H), 8.01 (d, *J* = 8.4 Hz, 1H), 7.97 (s, 1H), 7.90 (d, *J* = 8.4 Hz, 1H), 7.81 (s, 1H), 7.71 (s, 2H), 7.53 (t, *J* = 8.0 Hz, 1H), 7.40 (d, *J* = 3.2 Hz, 1H), 6.73 (dd, *J* = 3.6, 1.6 Hz, 1H), 5.08 (s, 1H), 1.54 (d, *J* = 6.8 Hz, 6H); MS (ESI) *m/z* calcd for C<sub>25</sub>H<sub>21</sub>N<sub>6</sub>O<sub>5</sub>S [M+H]<sup>+</sup> 517.1, found 517.1.

<sup>1</sup>H NMR spectrum of *N*-(5-(4-(methylamino)-3-nitrophenyl)-1,3,4-thiadiazol-2-yl)furan-2-carboxamide(**PT2(3A)**) (400 MHz, DMSO-*d*<sub>6</sub>)

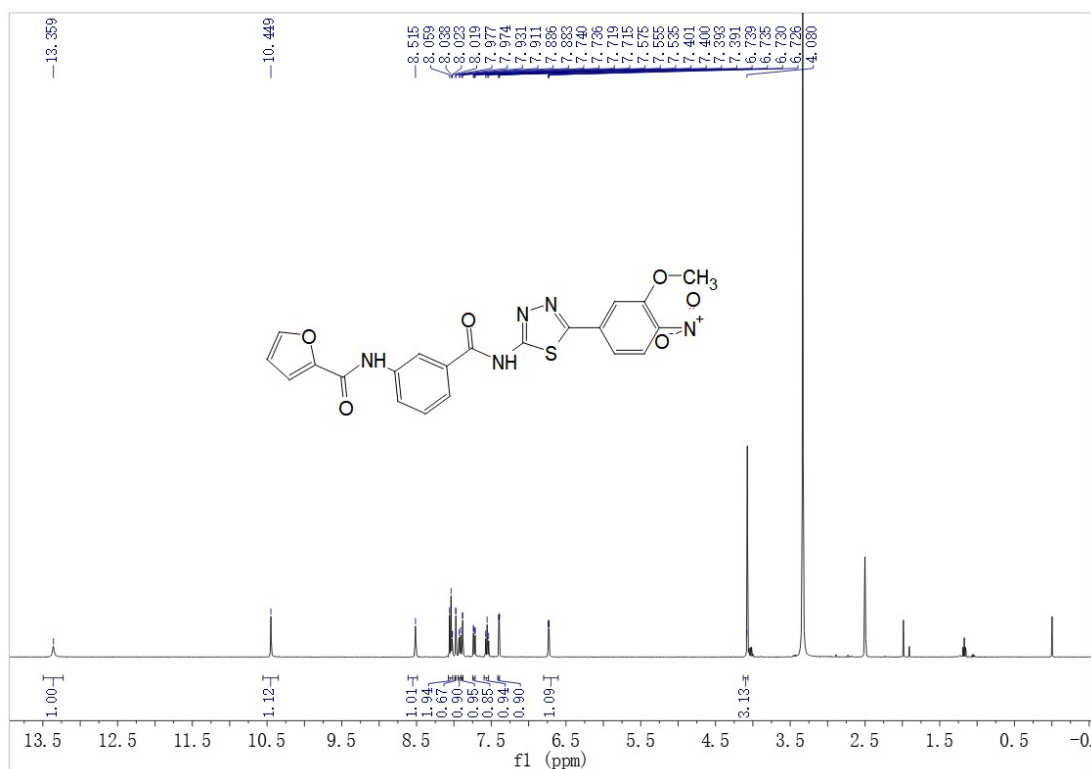


<sup>1</sup>H NMR spectrum of *N*-(3-((5-(4-(methylamino)-3-nitrophenyl)-1,3,4-thiadiazol-2-yl)carbamoyl)phenyl)furan-3-carboxamide (**PT5(3B)**) (400 MHz, DMSO-*d*<sub>6</sub>)

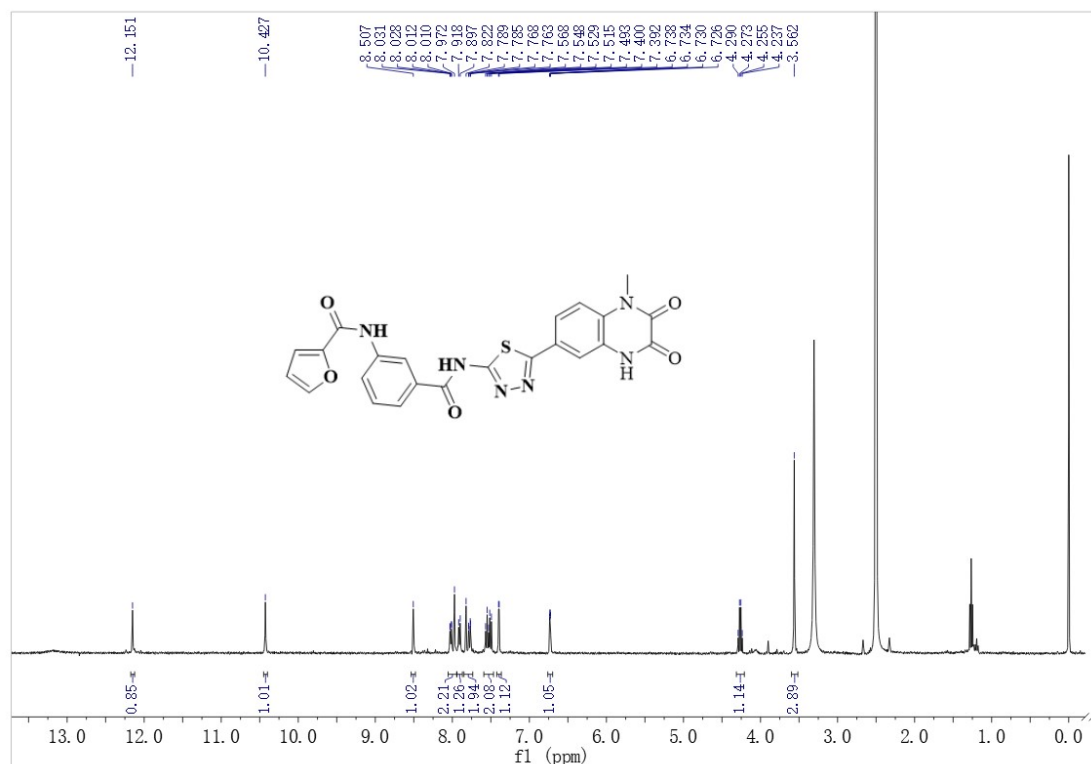


<sup>1</sup>H NMR spectrum of *N*-(3-((5-(3-methoxy-4-nitrophenyl)-1,3,4-thiadiazol-2-yl)carbamoyl)phenyl)furan-3-carboxamide (**PT5(3B)**) (400 MHz, DMSO-*d*<sub>6</sub>)

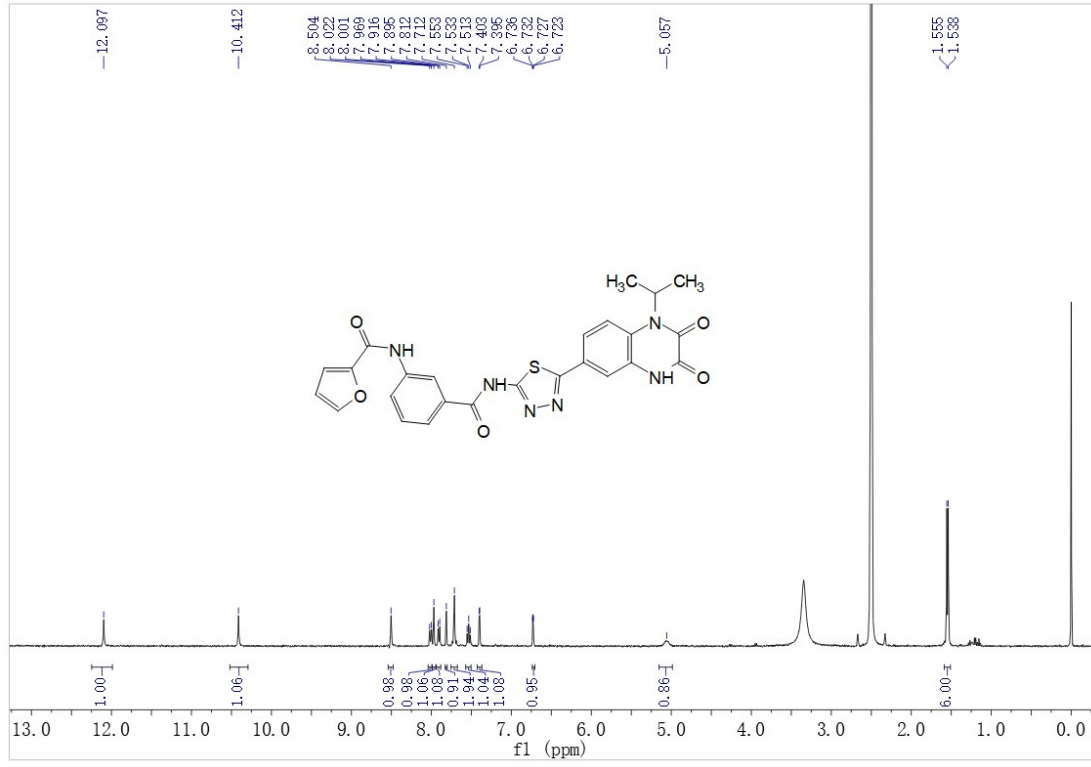
nyl)furan-2-carboxamide(**PT8(3C)**) (400 MHz, DMSO-*d*<sub>6</sub>)



<sup>1</sup>H NMR spectrum of *N*-(3-((5-(1-methyl-2,3-dioxo-1,2,3,4-tetrahydroquinoxalin-6-yl)-1,3,4-thiadiazol-2-yl)carbamoyl)phenyl)furan-2-carboxamide(**PT9(4A)**) (400 MHz, DMSO-*d*<sub>6</sub>)



<sup>1</sup>H NMR spectrum of *N*-(3-((5-(1-isopropyl-2,3-dioxo-1,2,3,4-tetrahydroquinoxalin-6-yl)-1,3,4-thiadiazol-2-yl)carbamoyl)phenyl)furan-2-carboxamide(**PT10(4B)**) (400 MHz, DMSO-*d*<sub>6</sub>)



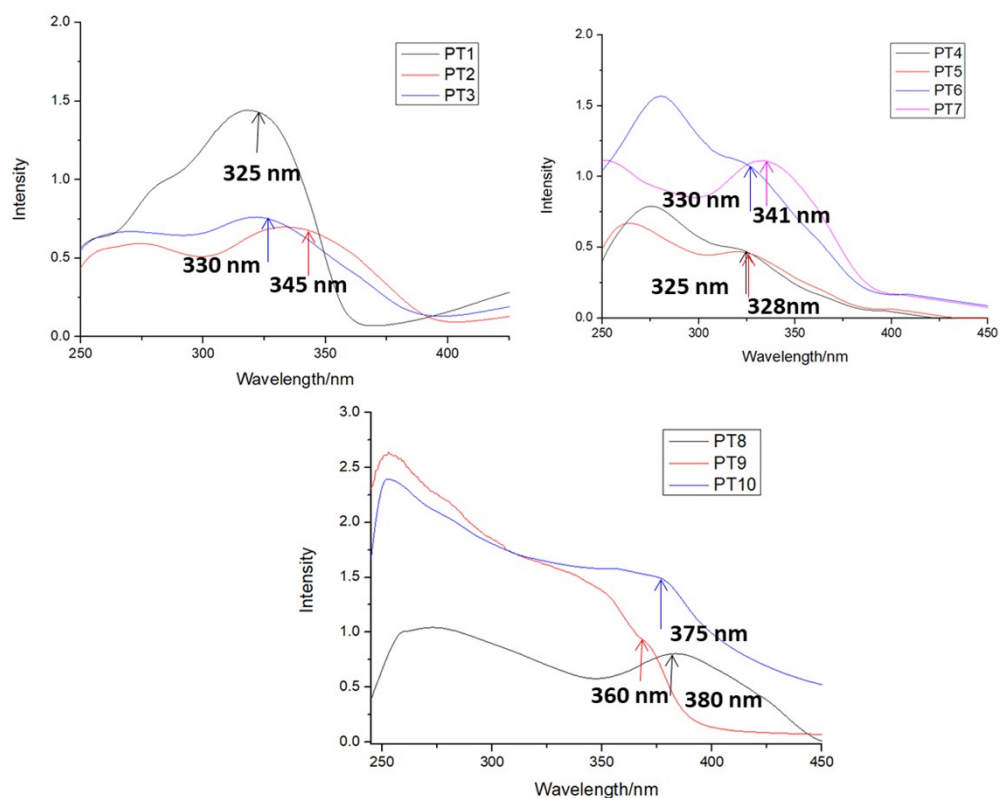


Figure S3. The UV excitation spectra of PT1– PT10 in PBS buffer (PBS: DMSO = 9:1) with a concentration of  $1.0 \times 10^{-4}$  M.

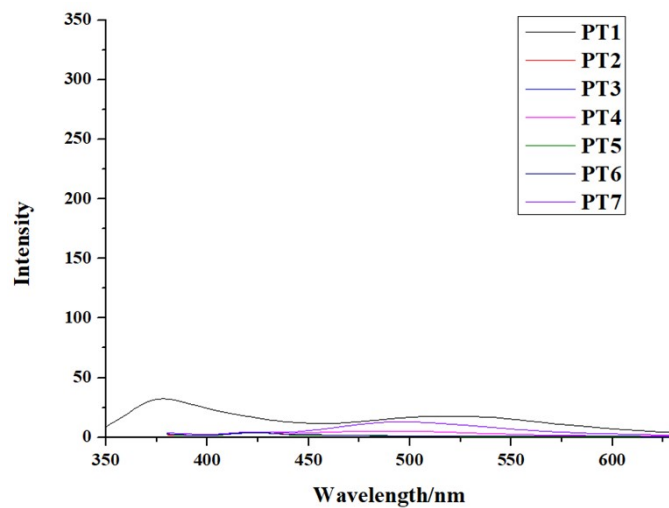


Figure S4. Fluorescence emission spectra of PT1- PT7 in PBS buffer (PBS: DMSO = 9:1) with a concentration of  $1.0 \times 10^{-4}$  M by excitation at 330 nm, 350 nm, 330 nm, 330 nm, 330 nm, 330 nm, 340 nm, respectively.

Table S9. Inhibitory activities of PT8, PT9 and PT10 against SHP1<sup>PTP</sup> and SHP2<sup>PTP</sup>, respectively.

Compounds	IC <sub>50</sub> (μM)	
	SHP1 <sup>PTP</sup>	SHP2 <sup>PTP</sup>
PT8	2.07±0.25	3.45±0.21
PT9	47.15±10.25	>100
PT10	51.09±7.06	83.43±4.55
NSC87877	5.81±0.26	3.85±0.32

NSC87877 (*Biochem. Bioph. Res. Co.*, **2009**, 381, 491-495) is a broad-spectrum phosphatase inhibitor as positive control and a high cited inhibitor of SHP2<sup>PTP</sup> and SHP1<sup>PTP</sup>. The IC<sub>50</sub> > 100 can be considered no inhibitory effect.

The IC<sub>50</sub> value of NSC87877 depends on the substrate, buffer pH, buffer components and incubation time (*Mol. Pharmacol.* **2006**, 70, 562–570; *Biochem. Bioph. Res. Co.* **2009**, 381, 491–495). In the time dependent/independent inhibition experiment (Figure S5), SHP1<sup>PTP</sup> were incubated with NSC87877 for different times. The results demonstrated that the IC<sub>50</sub> value of NSC87877 decreased with the increase of incubation time, indicating that NSC87877 is a slow-binding inhibitor for SHP1<sup>PTP</sup>. In order to match the fluorescence experiment, the incubation time was one hour in this experiment and different from 10 minutes in our previous work (*Chin. J. Org. Chem.* **2021**, 41, 3097–3105).

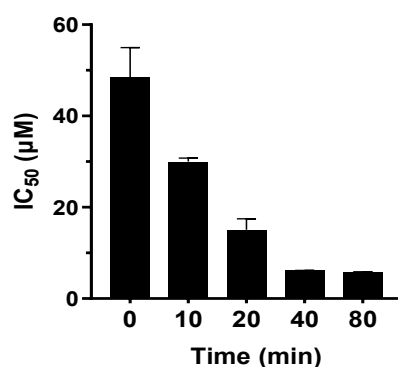


Figure S5. Time dependent/independent inhibition for SHP1<sup>PTP</sup> by NSC87877.

For enzyme activity imaging with 360 nm excitation wavelength, we obtained the fluorescent properties of PT9 under the concentration of 100  $\mu\text{M}$  and 10  $\mu\text{M}$  at room temperature. Measurements were performed in a reaction volume of 50  $\mu\text{L}$  using 384-well assay plates. In a typical 50  $\mu\text{L}$  assay mixture 60 mM HEPES, pH 7.2, 75 mM NaCl, 75 mM KCl, 1 mM EDTA, 0.05% Tween-20, 5 mM DTT and recombinant SHPs. The SHPs were solubilized in the assay buffer (HEPES, PH 7.2) and in 10-fold dilution from 4000 nM, a total of 4 gradients. The signal was measured on a multimode plate reader (EnVision Multilabel Reader, Perkin Elmer) with an excitation wavelength ( $\lambda^{\text{Ex}}$ ) of 360 nm and the experimental results were shown in Figure S6.

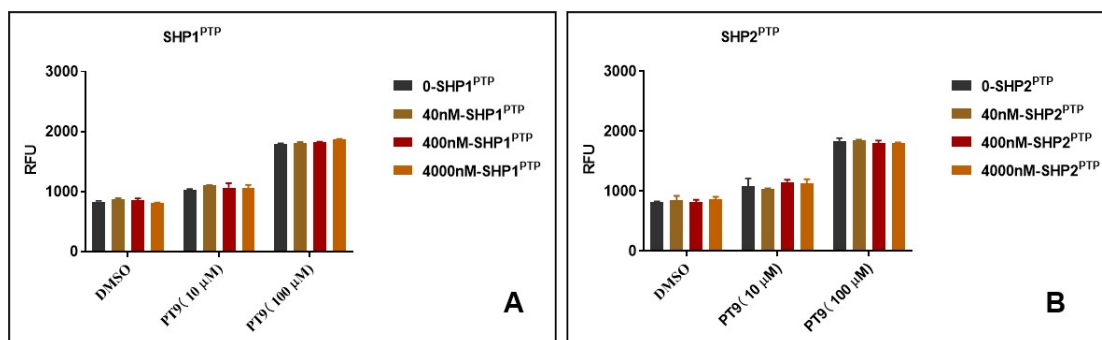


Figure S6. The fluorescence experiment of PT9 against the SHP1<sup>PTP</sup> and SHP2<sup>PTP</sup> enzyme activity.